



AGIP

STRA-ELSI

Seismic development and
Data Processing Depts.

OFFSHORE SICILY "G" ZONE

Notes on special seismic
data processing performed
on line G85-227/227A

R. Paganin - S. Gemelli

S. Donato Milanese, July 1988



INDEX

INTRODUCTION	1
SEISMIC DATA ACQUISITION	2
SEISMIC DATA PROCESSING	3
CONCLUSIONS	8
LIST OF FIGURES	9



.1

INTRODUCTION

This short note describes the seismic data processing carried out on the line G85-227 and part of the line G85-227A by AGIP-Elsi department on AGIP-Germ request, from February to June 1988.

Aim of this processing was the enhancement of the structural resolution of the seismic events pertaining to the East-Niobe structure, that gave the interpreter serious problems in finding the structural setting of horizons and faults in the previous section.

So, all this new stage of processing was completely devoted to solve this problem. A great number of programs was tested and this note explains the chosen processing sequence, our solution to the seismic structural problem.

The Niobe structure geographic location is shown in Fig. 1.



.2

SEISMIC DATA ACQUISITION

These are the principal acquisition parameters used to record the processed lines:

- Contractor.....: GEOITALIA, January-February, 1986
- Energy Source.....: Airgun, 2080 Cu.In., 4500 PSI,
average source depth 6 m;
- Spread Configuration: cable length 3187 m., offset 180,
number of groups 240, group interval
13.33 m;
- Magnetic Recorder...: LRS16A, format SEG-D, sampling interval 4
msec.;
- Field Filters.....: low cut 6 HZ ,high cut 87 HZ;
- Record Length.....: 4 sec.;
- Coverage.....: 12000 % .



.3

SEISMIC DATA PROCESSING

The Flow chart of the seismic data processing performed on the lines G85-227/227A is displayed on Fig. 2.

The main processing steps are the following:

1 - **Edit Floating Point** - Seismic data, acquired on field in multiplexed form, were demultiplexed and collected in Shot point Gatherers. Amplitudes were restored to the same recording level. From then on all the processing steps and outputs were handled using floating point notation in order to preserve the full dynamic range of the data.

2 - **Sort to CDP Gathers** - Input demultiplexed data were arranged in CDP ordered data and a preliminary stack was obtained (Fig. 4). At the same time all the data were compensated for amplitude decay. Geometrical spreading functions were derived from a preliminary amplitude decay analysis and converted into time and offset variant multipliers. All the traces were also balanced to a unique RMS mean value. Then, seismic data coming from line G85-227 and G85-227A were merged taking into account their topographic position. From this point on, the two lines were processed as a unique one.

3 - **Minimum phase conversion** - This processing step removes from seismic data the phase distortion due to the non-instantaneous response of the acquisition electric equipment. A phase shift operator was computed starting from the impulse response characteristic of the recorder used (LRS 16A) and of the field filters chosen (Low cut 6 Hz 18 Db/Oct, High cut 87 Hz 132 Db/Oct). A minimum phase equivalent wavelet was computed from this response and an operator was obtained with the Wiener-Levinson least squares shaping method by using the minimum phase equivalent wavelet as desired output. The computed operator was applied to the seismic data; this is the first step of the process that brings seismic data to minimum phase condition and data are ready to pass to the second step that is the spiking deconvolution.

Fig. 3 shows the dephasing operator computation.

4 - **Deconvolution Before Stack (DBS)** - A predictive deconvolution



.4

was applied to seismic data sorted to CDP gathers. After a great number of programs that tested the effect of changing of each parameter on seismic data, the values chosen were:

Prediction Distance: 4 msec.

Operator Length: 400 msec.

Computation Windows: 2 (0 - 2.3 and 2.3 - 4 sec.)

White Light Added: 10 %

The use of a Spiking Deconvolution was possible due to the good result of the previous step; so the minimum phase recovery of seismic data was completed: the previous step attacked the phase and amplitude delays due to known causes (recorder response), while this second step attacked those not recognizable, due to the propagation of seismic waves in a very complex media, whose effects are very difficult to estimate.

5 - Dip Move Out Correction (DMO) - This processing step is the most important pre-stack step in seismic structural processing. Lines with very dip seismic horizons are affected by a geometrical anomaly in the real positioning of reflections that give also an error in determining stacking velocities of related reflections. This error is proportional to the dip of the event. Of course, DMO correction is an indispensable step in seismic structural processing because we must firstly restore the exact positioning in time-space domain of the seismic reflections and also because the stacking velocities computed after DMO correction of the seismic data are not affected by an offset-dependent error and can be successfully used as seismic velocity information for the time migration. This particular kind of dynamic correction was applied on CDP gathers after a NMO correction, computed using a preliminary stacking velocity field, and a partial stack of adjacent traces, reducing the coverage from 12000 % to 6000 %. The reason of the NMO correction was only for the correct summing of adjacent traces; the reason for the reduction of coverage was only to get the program faster and more economic, because processed data are reduced by 50 %; moreover, the 6000 % coverage is yet sufficient for subsequent velocity analysis step. DMO algorithm was then applied on offset planes and then an inverse NMO correction was applied to leave the effects of a preliminary velocity field. On offset planes, a velocity filtering was also performed, erasing aligned noise with apparent velocity of 1500 m/sec. So seismic data were refined from noise travelling in water, without touching reflection and diffraction hyperbolae.

The effects of a DMO correction on seismic data are not always imme-



.5

diateley appreciable: normally there is a good increase in resolution of the dipping events and on the diffraction hiperbolas, but the good results of a DMO correction can be observed in the next steps of seismic data processing, such as Stacking Velocity Analysis and Time Migration.

In Fig. 6 is displayed the Stack after DBS and DMO correction in the target zone.

6 - Stacking Velocity Analysis - After DMO correction, a stacking velocity analysis was performed on CDP ordered data. Along the line 30 analyses were positioned to investigate in the main interesting zones, so to have a velocity field that could give us all the information we need for the NMO correction and for the time migration. The analysis methods used were the Costant Velocity Stack on 8 CDF's and the cross-correlation matrix display.

The velocity analysis parameters used are:

Mean Spacing: 300 - 500 m.

Number of CDF's used: 8

Velocity range: 1500 - 5000 m/sec.

Velocity increment: 100 m/sec.

Correlation Gate: 0.0 - 2.0 sec. - 24 msec.
2.0 - 4.0 sec. - 48 msec.

Fig. 5 shows an example of velocity analysis after DMO correction.

7 - NMO correction and Stack - All the CDP gathers were NMO corrected and stacked using the interpreted stacking velocities. After NMO correction, the early times of the traces were muted of the stretched amplitudes; the mute function was controlled and changed along the section to follow the structural changes of the events.

8 - Minimum to zero phase conversion - Average amplitude spectra were extracted from Stack section on windows over the target zone that gave us the statistical minimum phase wavelet estimated from that data (Fig. 7). Subsequently, statistical least squares operators which transform the computed wavelets into their zero phase equivalent were obtained (Fig. 8). Seismic data were filtered with those operators. Bringing signal from minimum to zero phase is a very useful tool for data interpretation because peaks and troughs can be directly related



to acoustic impedance contrasts for lithological changes. Moreover, among all the wavelets with a specified amplitude spectrum, the zero phase wavelet has better resolution.

In Fig. 9 is shown the zero phase Stack in the target zone.

9 - Time Variant Filtering (TVF) - A final filtering operation was applied on zero phase stack in order to improve the quality of seismic data. Some time and space varying windows were designed in order to divide data in homogeneous frames and following them along the section. The choice of the filtering parameters, (high cut and low cut), was performed with a previous frequency coherence analysis. This kind of analysis, performed with a comparison of frequencies of adjacent traces, can discriminate with a good degree of confidence what are the limits in frequency of the signal. In fig. 11 is displayed the comparison between the final stack of the agip processing and the previous one.

10 - Time Migration - Final Stack was then time migrated to remove diffracted energy and restore the real position of reflections in Time - Space domain (Fig. 10). After testing various algorithms, the migration chosen was the W-X Domain Time Migration. This algorithm can successfully handle dips to nearly 80-90 degrees and velocity variations, either in lateral or vertical directions.

Also if working in Frequency domain simplifies the computation, the program is more expensive than the other algorithms, but the increase in costs is compensated by the increase in structural resolution of the seismic data. In Fig. 12 is displayed the comparison between the final migration of the Agip processing and the previous one.

11 - Seismic Velocity Modelling - Seismic Interval Velocity Field computation is the first stage of the Depth Migration step. The differences between this and the time migration field are in the reference domain. For time migration the velocity should be specified as Space - Time function, while for depth migration they should be specified as Space - Depth function. The reason of these differences must be found in the depth migration algorithm and will be explained in the depth migration step.

Input data of this processing step are all the velocity information available and a first seismic horizon interpretation. In this case the velocity information used consist in the formation velocities resulting from well velocity logs studied in that area. These interval velocities were distributed along the section according with interpreted horizons (from stack section), by using an interactive



velocity modelling program specially designed for the time and depth migration velocity fields computation. This program can compute, modify and interpolate velocity information and can test the velocity field with forward modelling ray tracing routines, comparing input time horizons and corresponding synthetic ones. In Fig. 13 and 14 are displayed the time model used for Seismic Velocity Modelling and the output RMS velocity field computed for Depth Migration.

12 - Depth Migration - The final Velocity Field was then used for the Depth Migration (Fig. 15). The algorithm used was always the W-X one, like the Time Migration. This kind of migration, in fact, can successfully operate either in Time or in Depth Domain. In particular, Depth Migration algorithm computes depth traces directly from the Stack data. The seismic wavefront propagation is reconstructed taking into account the Snell's law lowering progressively the source-to-receiver pairs deeper and deeper until they reach the maximum depth of interest. At any level of this downward continuation, the data above the sources and receivers depth positions are fully migrated into depth and the data below are referred to the unmigrated time section that should have been recorded at that source-receiver depth. So, the processing goes on step by step migrating directly in depth the Stack section. Also this algorithm works in frequency domain with an implicit finite difference formulation. The depth values of the seismic section resulting from this operation cannot be of course considered as absolutely exact, because of the absence of control points such as well data informations, but certainly they can give us an idea of the geological setting in depth of the target structure. Nevertheless, the Depth Section was refined by iterating the velocity model computation and the Depth Migration in order to increase the detail of the velocity model after the interpretation of the intermediate depth migration steps.



.8

CONCLUSIONS

As explained before, all the seismic data processing steps were oriented to increase the structural resolution of the target structure. So we tried to delineate a processing sequence to solve structural problems. For this purpose, all the most up-to-date programs have been used. The results of this processing might be considered satisfactory, taking into account that no well data were used to calibrate velocity and depth information, and only a seismic line was used. But surely these results encourage to continue the processing involving seismic lines around the geologic structure and the well located in the zone. In fact the work done can be easily used as a guide for the seismic processing of a large grid of lines to better delineate in three dimensions the complex geologic structure "East Niobe".



LIST OF FIGURES

- Fig. 1 Niobe structure geographic location.
- Fig. 2 Seismic data processing flow chart.
- Fig. 3 Minimum phase dephasing operator computation.
- Fig. 4 Preliminary Stack in the target zone.
- Fig. 5 Example of Velocity Analysis after D.M.O. correction.
- Fig. 6 Stack after Decon and D.M.O. correction in the target zone.
- Fig. 7 Frequency content analysis on Stack for Minimum Phase wavelet estimate.
- Fig. 8 Minimum to Zero Phase operator computation.
- Fig. 9 Zero Phase Stack in the target zone.
- Fig. 10 Time Migration in the target zone.
- Fig. 11 Final Stack comparison.
- Fig. 12 Final Migration comparison.
- Fig. 13 Time model for Seismic Velocity Modelling.
- Fig. 14 RMS Velocity field for Depth Migration.
- Fig. 15 Final Depth Migration (W-X Domain).

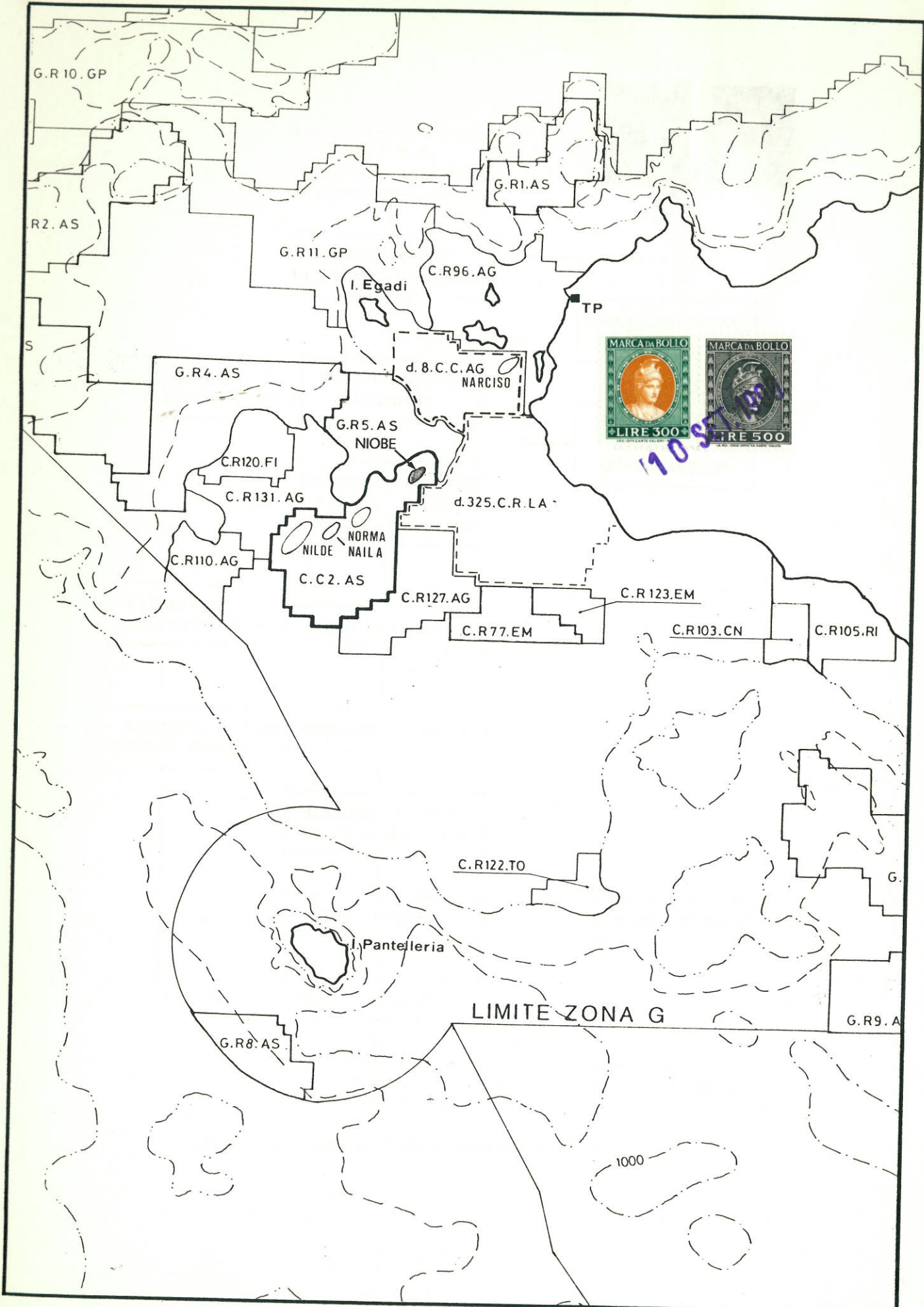


Fig. 1 NIOBE STRUCTURE GEOGRAPHIC LOCATION

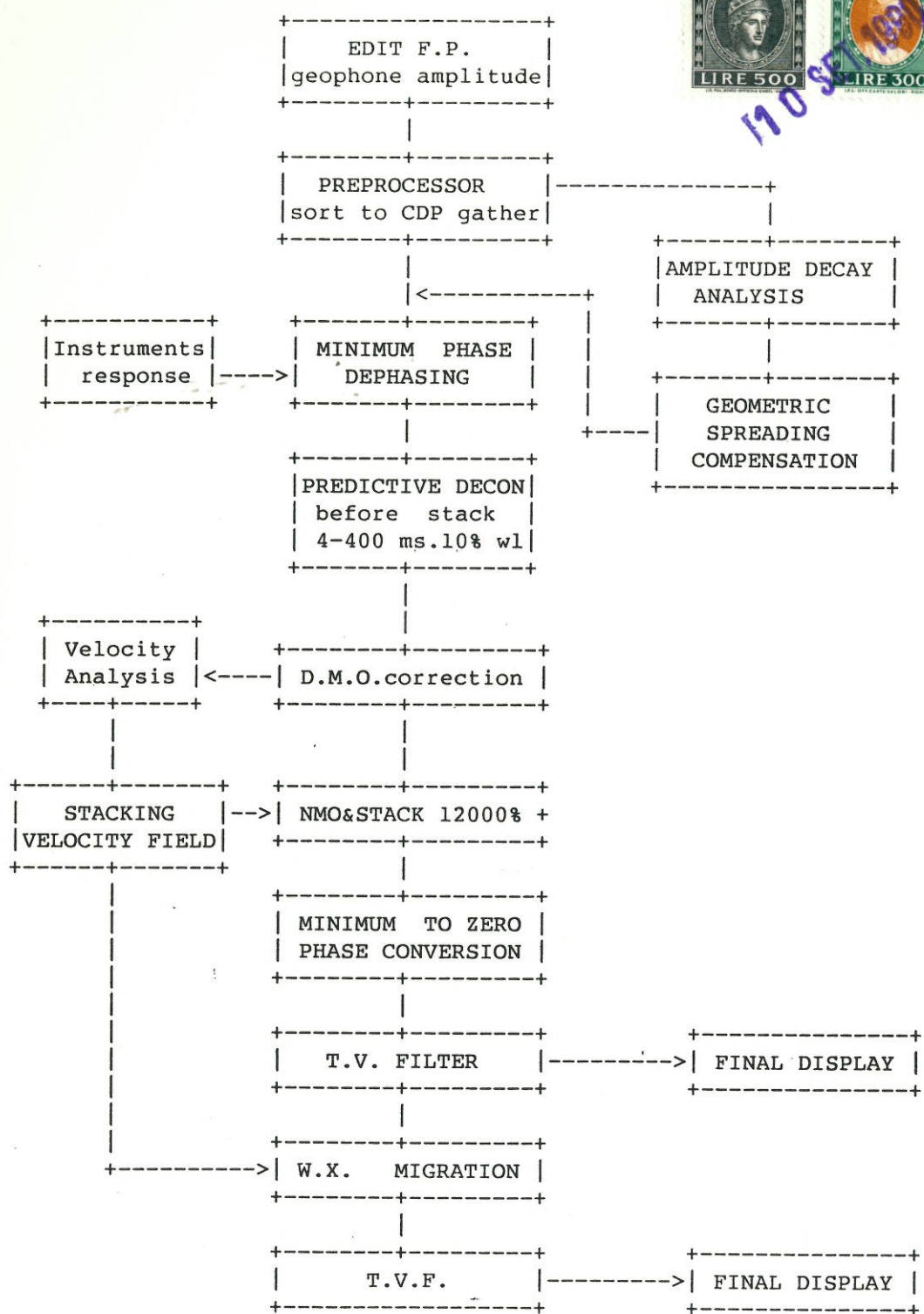


Fig. 2: Seismic data processing flow chart

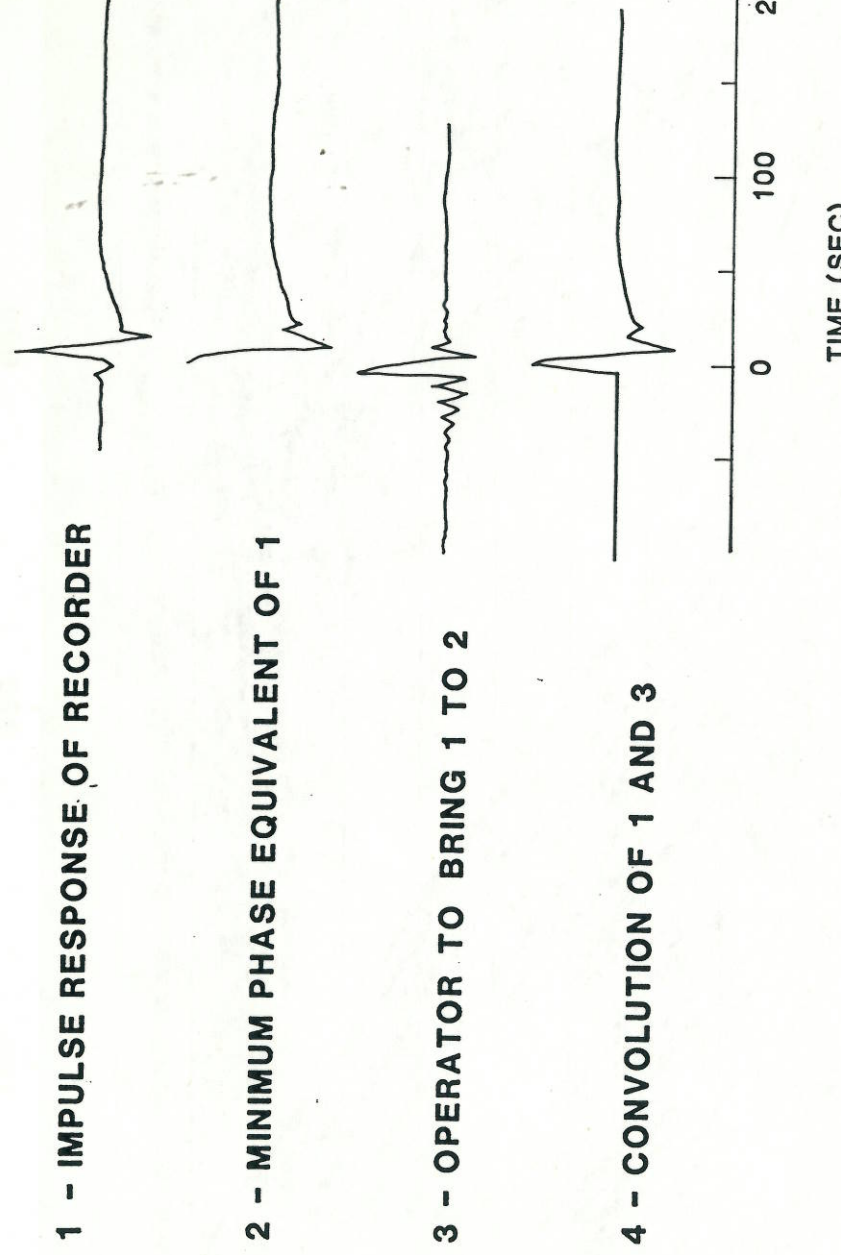


Fig. 3 Minimum phase dephasing operator computation



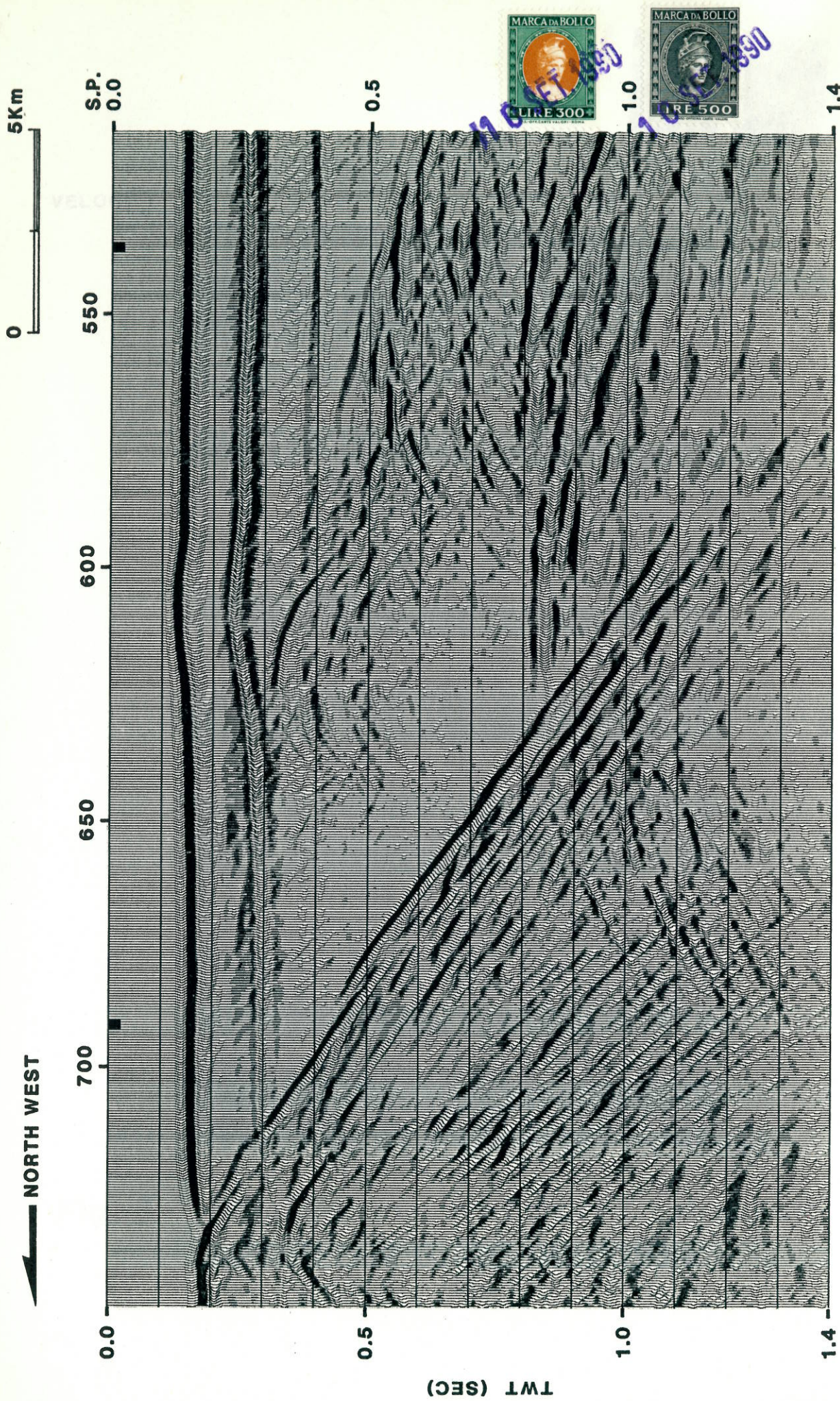
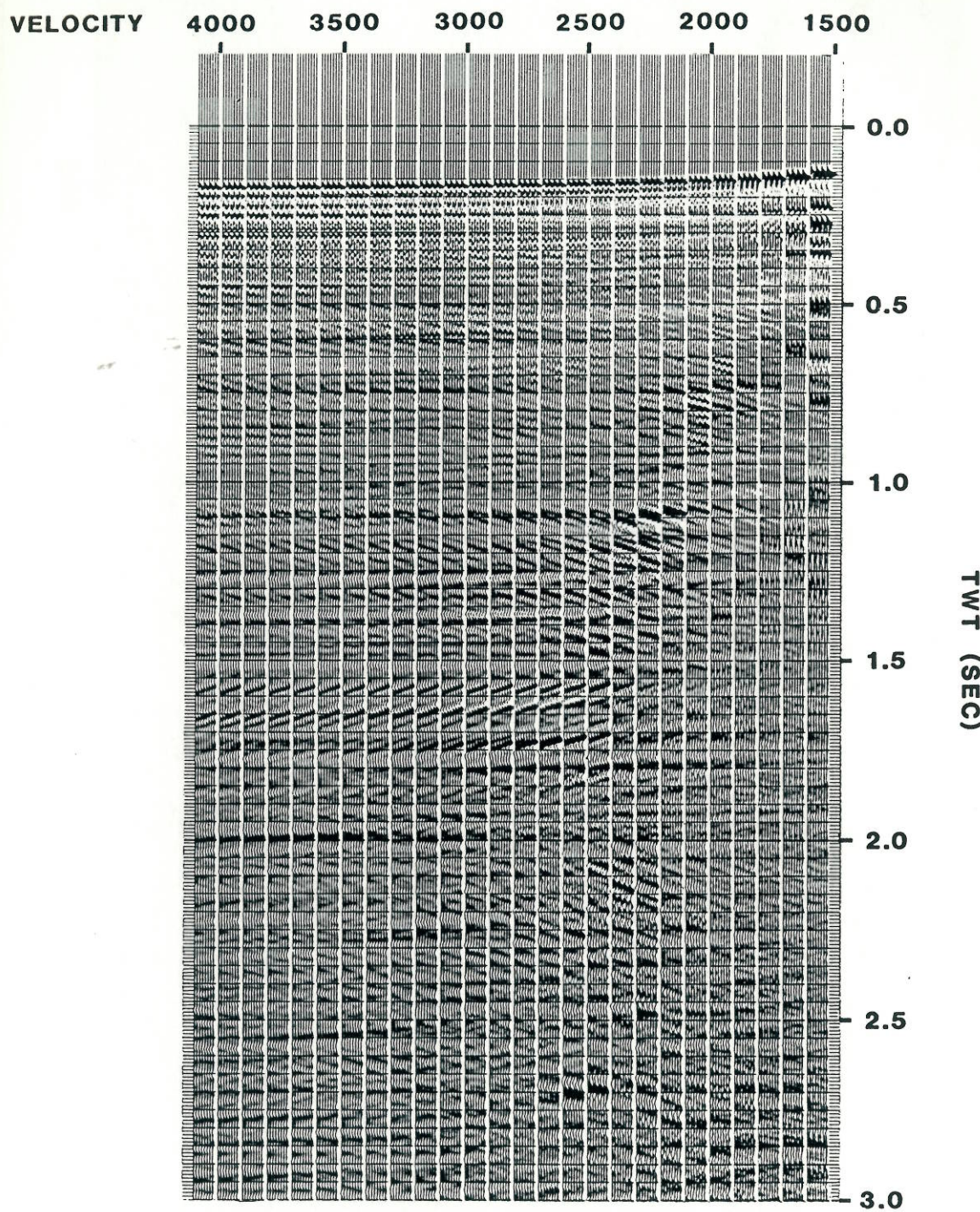


Fig. 4 PRELIMINARY STACK IN THE TARGET ZONE



**Fig. 5 EXAMPLE OF VELOCITY ANALYSIS
AFTER D.M.O. CORRECTION**

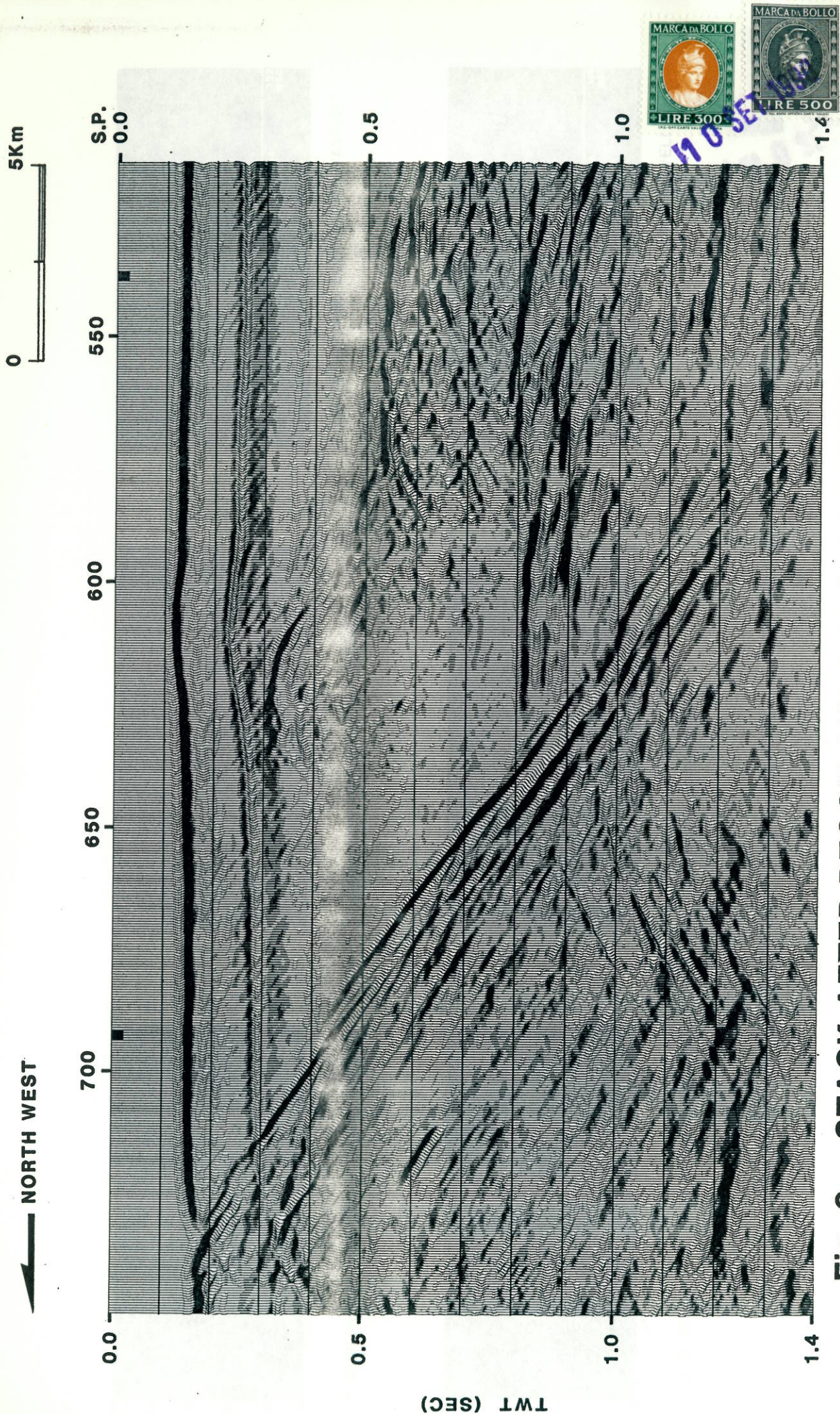
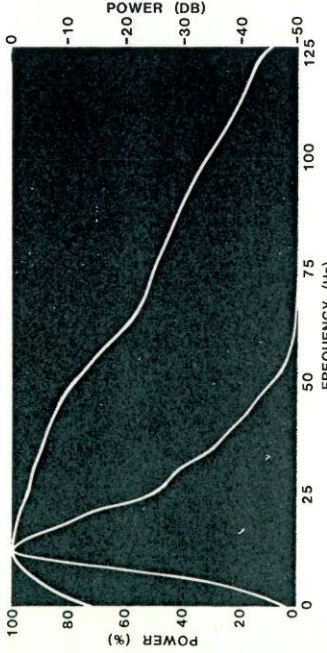
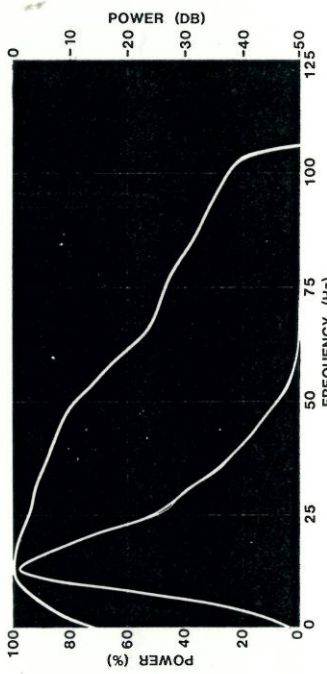


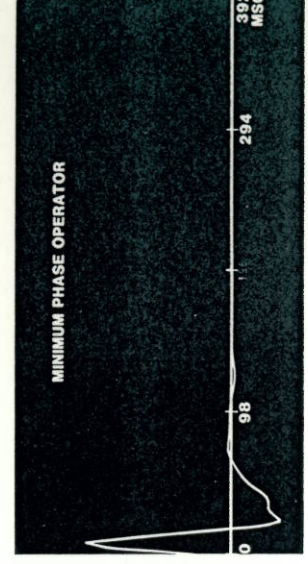
Fig. 6 STACK AFTER DECON AND D.M.O. CORRECTION IN THE TARGET ZONE



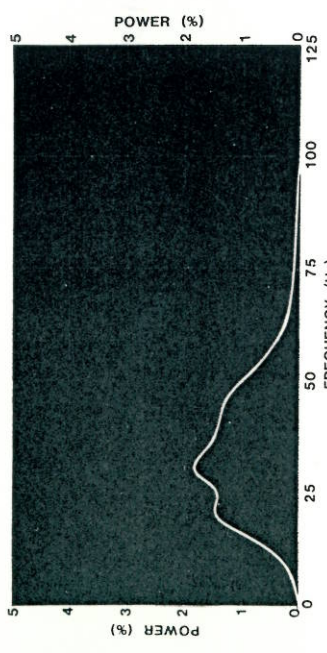
1 AMPLITUDE SPECTRUM OF SIGNAL + NOISE



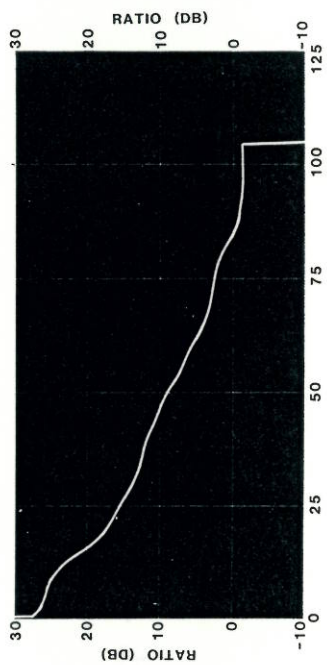
2 AMPLITUDE SPECTRUM ON SIGNAL



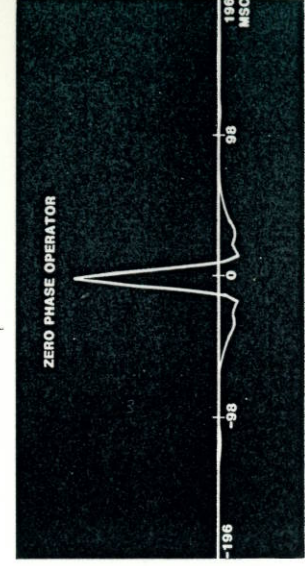
3 MINIMUM PHASE EQUIVALENT WAVELET



4 AMPLITUDE SPECTRUM OF RANDOM NOISE



5 S/N RATIO SPECTRUM



6 ZERO PHASE EQUIVALENT WAVELET
NO SET. NO

Fig. 7

FREQUENCY CONTENT ANALYSIS ON STACK FOR MINIMUM PHASE WAVELET ESTIMATE



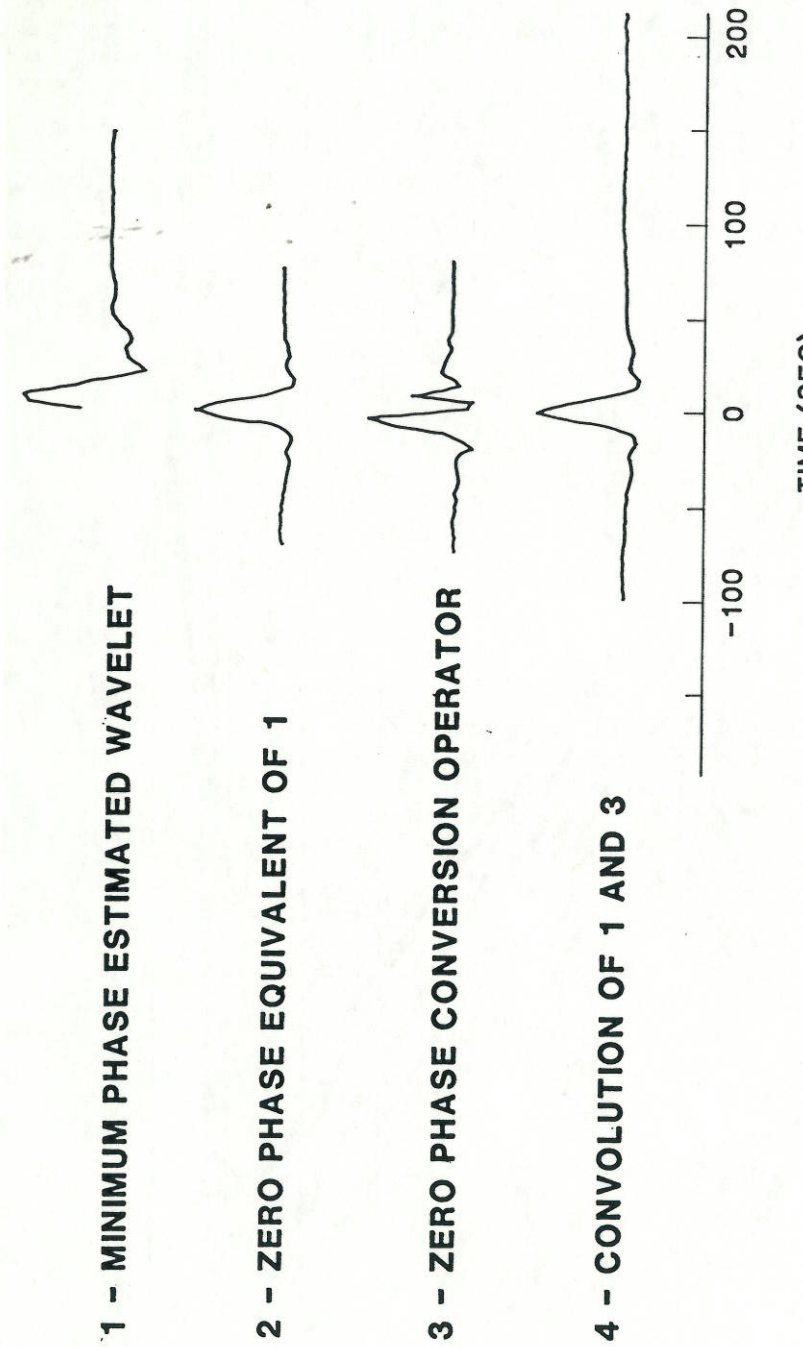


Fig. 8 Minimum to zero phase operator computation

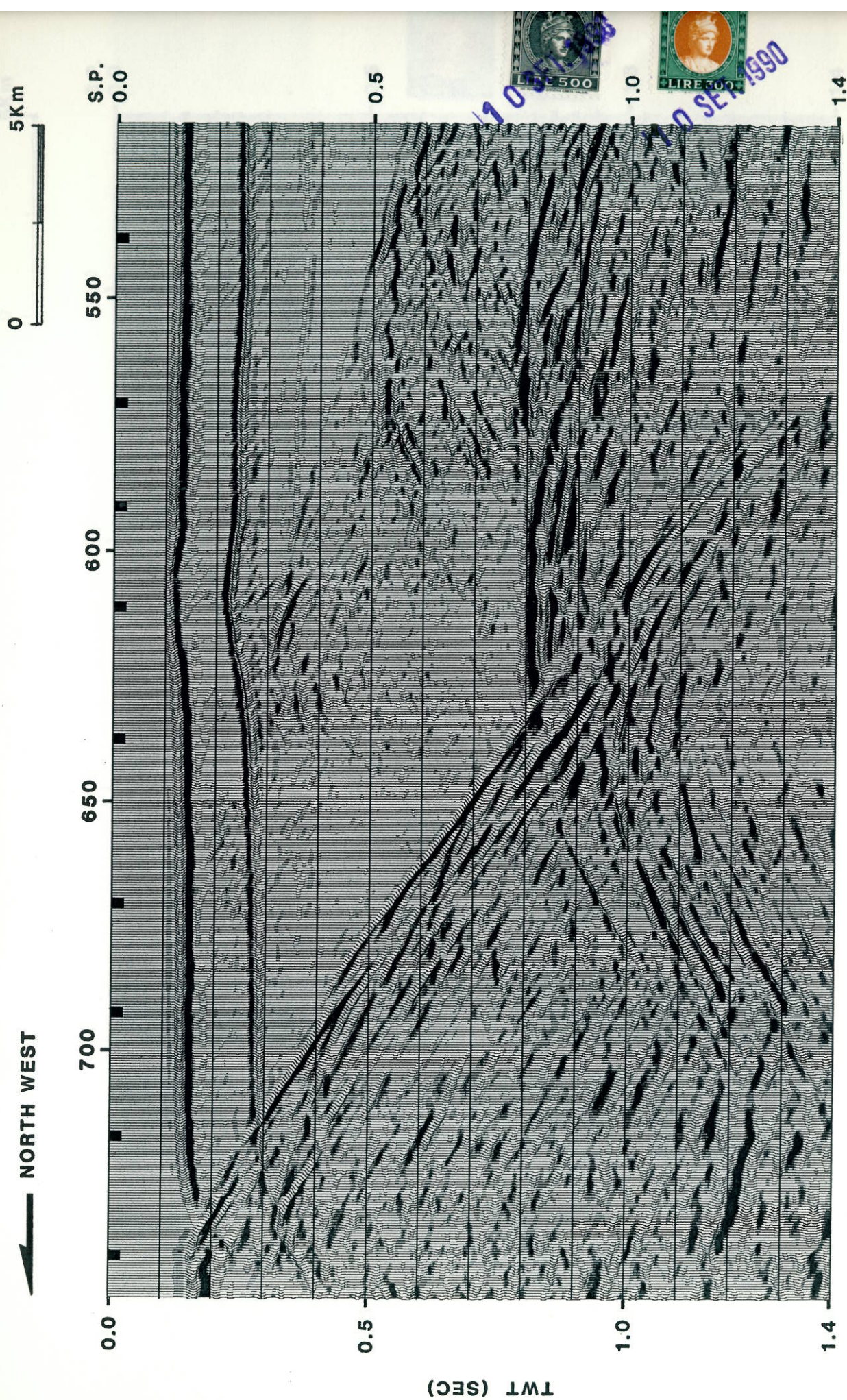


Fig. 9 ZERO PHASE STACK IN THE TARGET ZONE

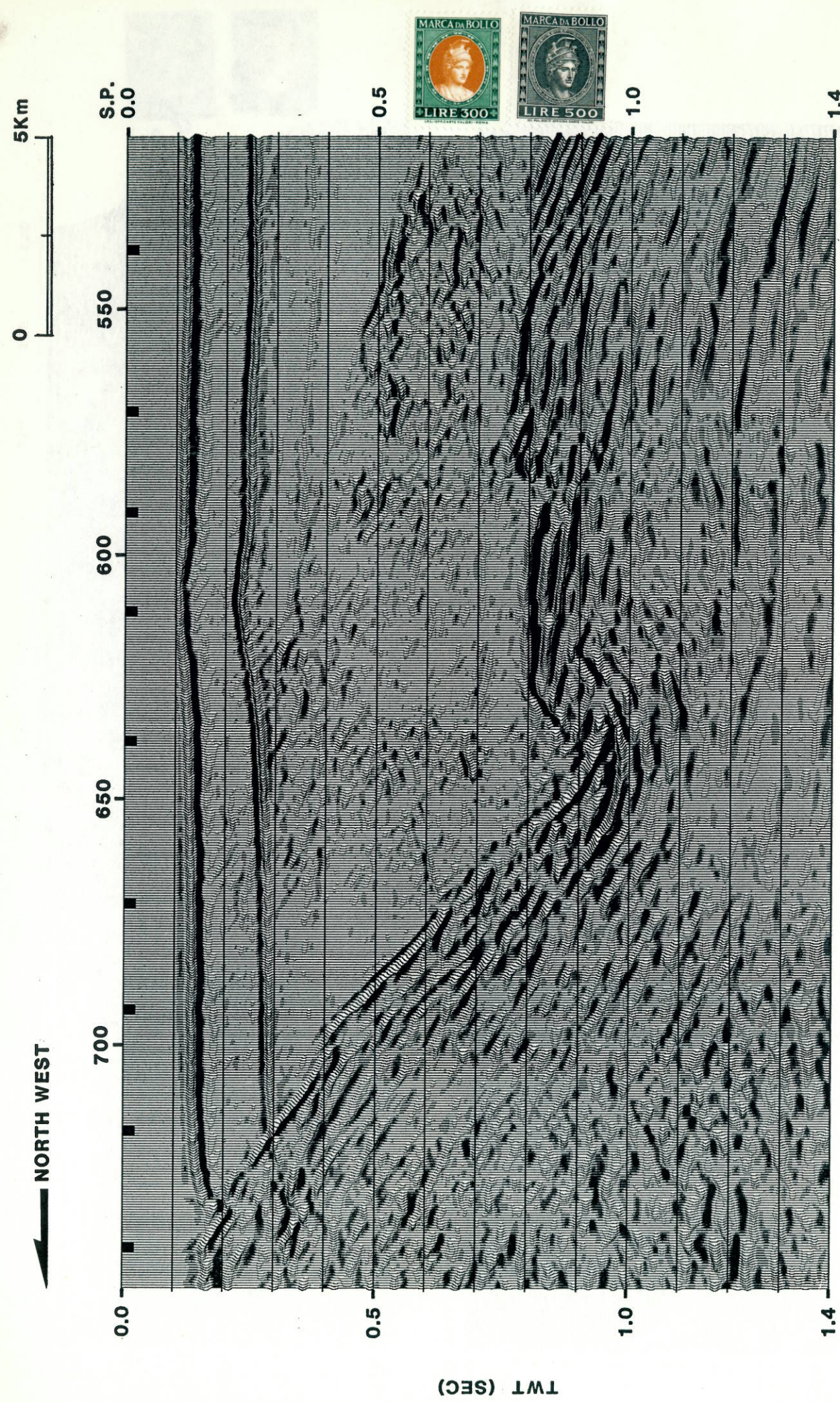
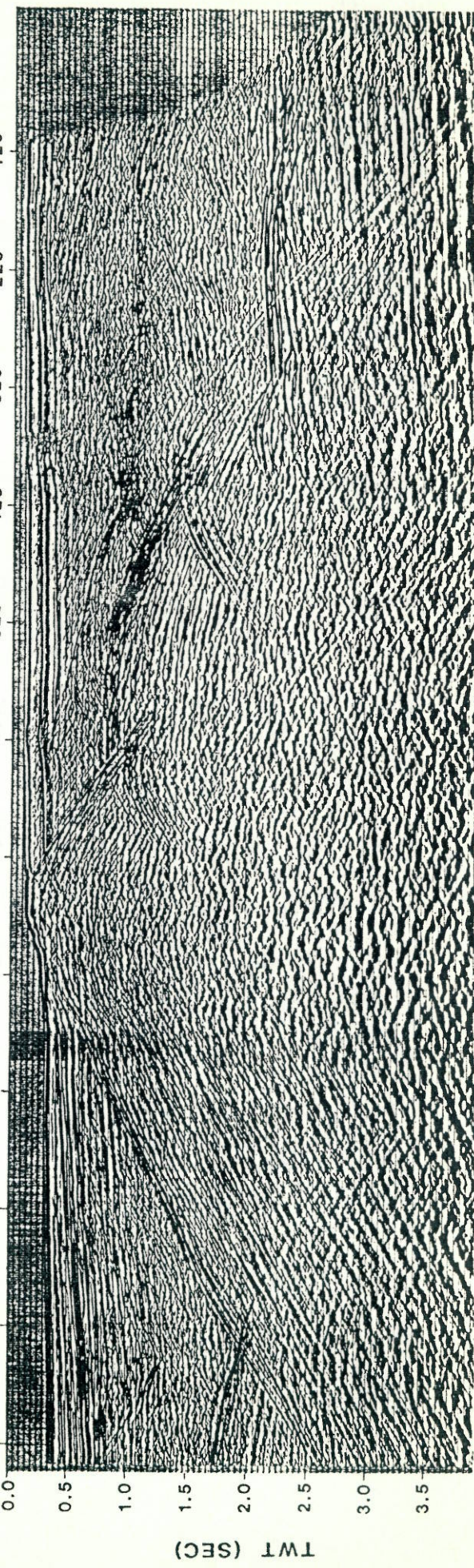
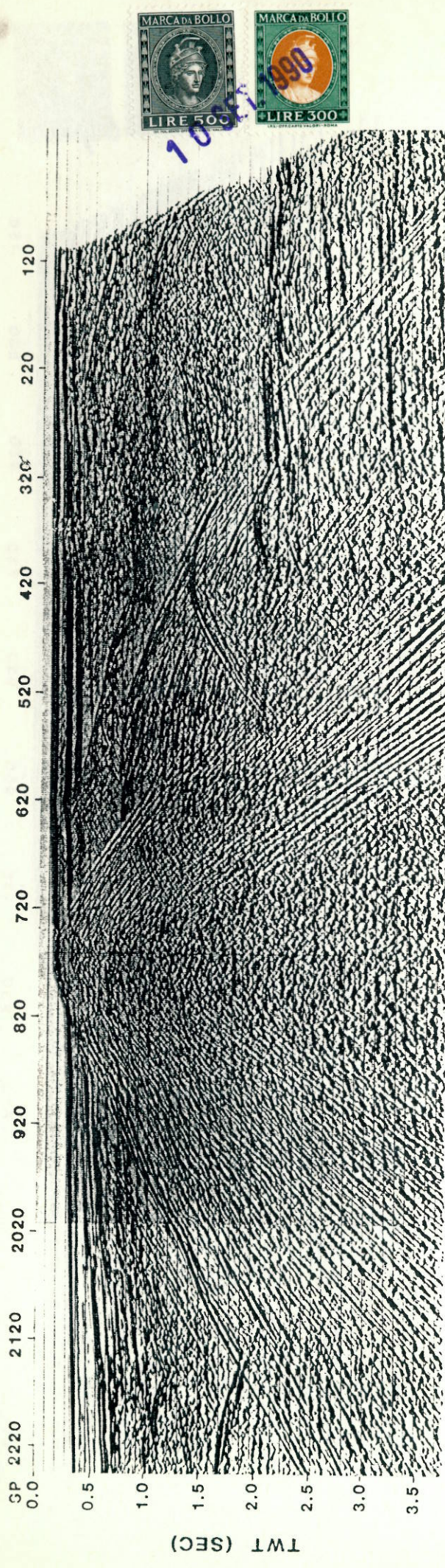


Fig. 10 TIME MIGRATION IN THE TARGET ZONE



AGIP PROCESSING
Fig. 11 FINAL STACK COMPARISON

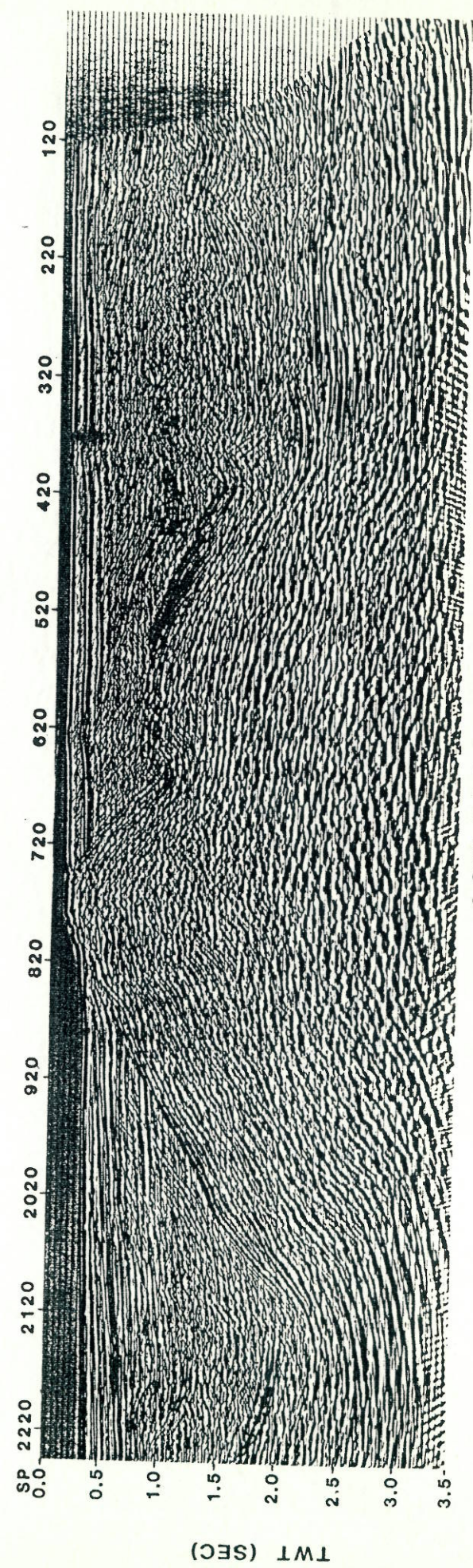
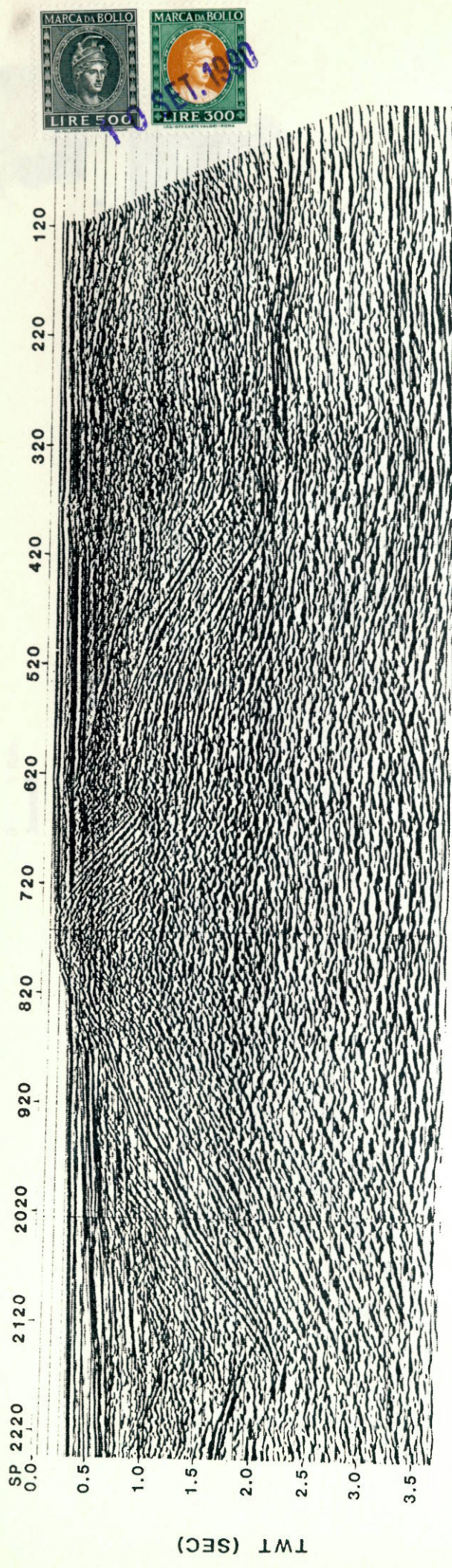


Fig. 12 FINAL MIGRATION COMPARISON

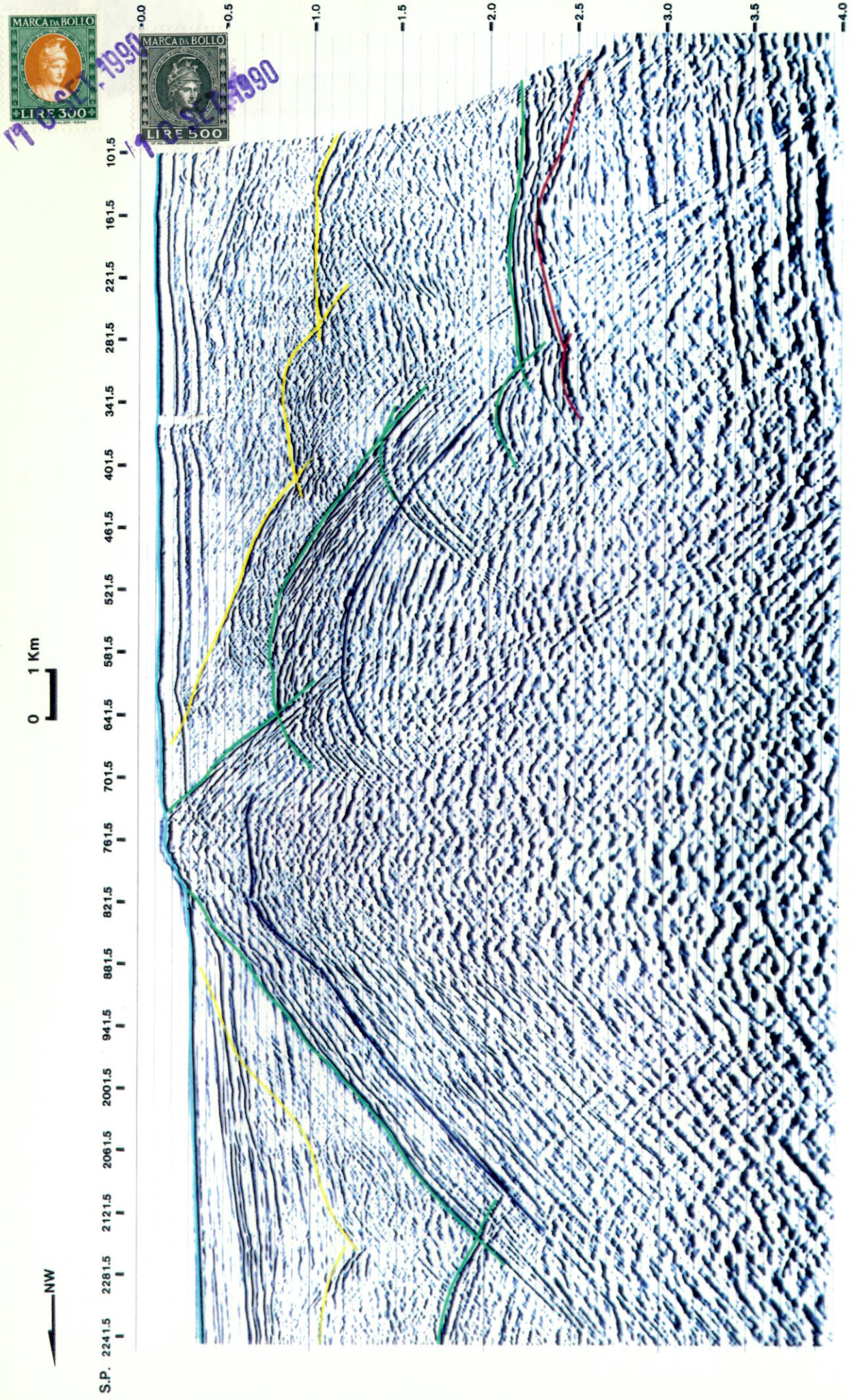


Fig. 13 TIME MODEL FOR SEISMIC VELOCITY MODELLING

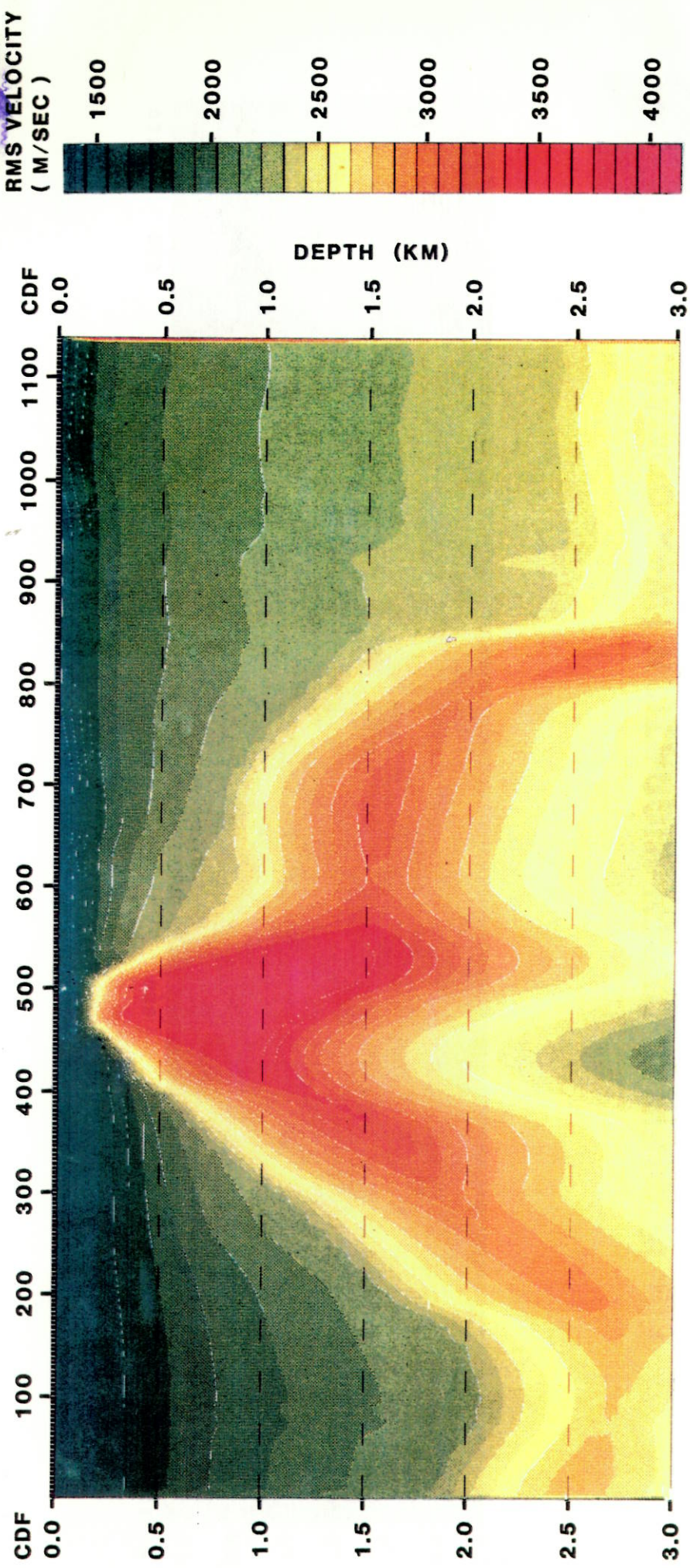


Fig. 14 RMS VELOCITY FIELD FOR DEPTH MIGRATION

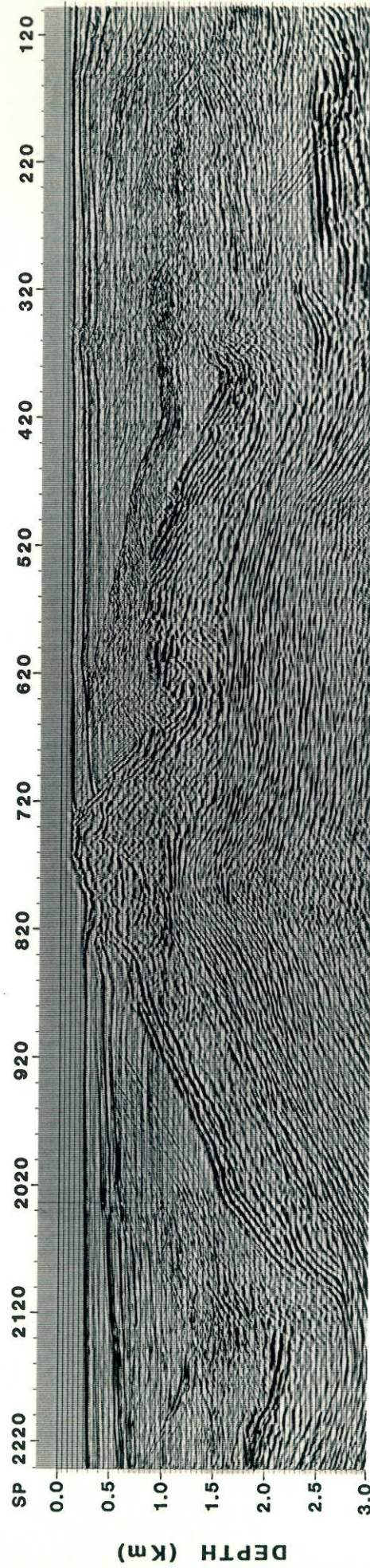


Fig. 15 FINAL DEPTH MIGRATION (W-X DOMAIN)